

Topological Quantities: Calculating Winding, Writhing, Linking, and Higher order Invariants

Mitchell A. Berger
(CIME Lecturer)

Abstract Many topological calculations can be done most easily using the basic idea of *winding number*. This chapter demonstrates the use of winding number techniques in calculating writhe, linking number, twist, and higher order braid invariants. The writhe calculation works for both closed and open curves. These measures have applications in molecular biology, materials science, fluid mechanics and astrophysics.

1 Introduction

Often we can find several equivalent expressions for a mathematical quantity. One of these may seem most fundamental, and so may be chosen to be the definition of the quantity. Other expressions can prove useful in proving theorems or in calculations. This chapter considers geometrical quantities associated with curves, such as twist, writhe, linking numbers and higher order invariants.

For all these quantities we can obtain expressions based on the fundamental idea of *winding number*. This chapter will show how winding number techniques simplify and speed up calculations, and add insight into what the quantities actually measure.

Objects such as knots and links are fundamentally three-dimensional – and yet many knot invariants rely on almost two-dimensional representations. The usual method involves projecting knotted curves onto a plane. Information about the third dimension only survives at crossings: at places where one

M.A. Berger
Mathematics Dept., SECAM, University of Exeter,
North Park Rd. Exeter EX4 4QE, U.K.
e-mail: m.berger@exeter.ac.uk
<http://secamlocal.ex.ac.uk/people/staff/mab215/home.htm>

part of a curve crosses under or over another part we specify which curve is on top. Invariants can then be deduced by examining the pattern of over and under-crossings.

This chapter investigates a less severe reduction of dimensionality. Here one direction (which we will generally take to be the z direction) is singled out. Suppose s measures arclength along a curve. Then a three-dimensional curve can be parameterized by s , and specified by the three coordinate functions $(x(s), y(s), z(s))$. If, however, $z(s)$ is a monotonic function of s , i.e. the curve always travels upwards (or downwards) in z , then we could parameterize by z instead. Now we need only two coordinate functions – $(x(z), y(z))$. This considerably simplifies calculations. Also, this procedure immediately makes a connection with two-dimensional dynamics: simply replace the letter z with the letter t , symbolizing time. The 3-D curve $(x(z), y(z), z)$ becomes the time history (space-time diagram) $(x(t), y(t), t)$ of a point moving in the $x - y$ plane.

The reader may already be objecting that most curves (certainly all closed curves) are not monotonic in z : they go up and down. To deal with this simple fact, we will have to chop up our curves at turning points where $dz/ds = 0$ (see figure 1). This is the price we must pay for the reduction from three coordinate functions to two. We will now have to sum over all the pieces of our curves when we wish to calculate something like writhe or linking number.

In many applications a special direction is already singled out. For example, elastic rod experiments sometimes fix the rod between parallel planes. In some astrophysical applications, one considers the geometry and topology of magnetic field lines anchored at a boundary surface. This surface might be

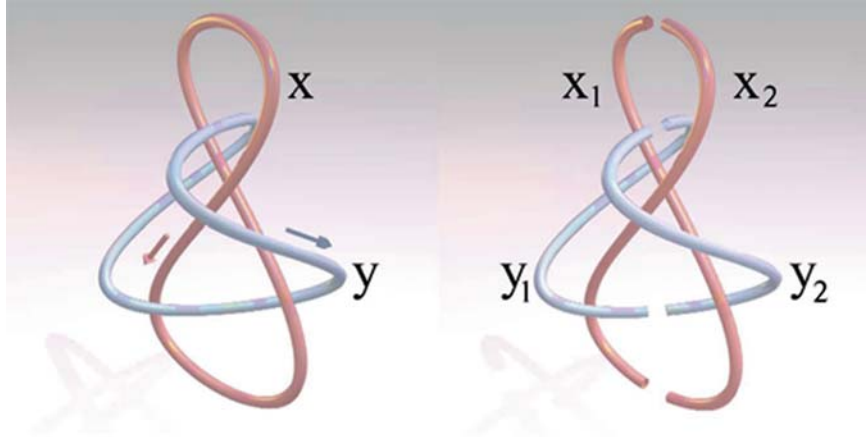


Fig. 1 On the left, a Whitehead link consisting of two curves $\mathbf{x}(t)$ and $\mathbf{y}(t)$. Arrows give the directions of the curves, i.e. the directions of increase of arclength s . On the right, the curves have been chopped into sections $\mathbf{x}_1, \mathbf{x}_2$ and $\mathbf{y}_1, \mathbf{y}_2$ at their maxima and minima in z .

the photosphere of the sun or the surface of an accretion disk. In the solar case z should be replaced by radial coordinate r . In other applications we start with a time history of the two-dimensional motion of several objects (e.g. [KHS06, GVV03]). In the corresponding space-time diagram the curves $(x(t), y(t), t)$ twist and braid about each other; the topology and geometry of this braiding gives information about the dynamics.

2 Winding Numbers

2.1 Two Braided Curves between Parallel Planes

First consider two curves stretching between parallel planes (see figure 2) separated by a height h . Let these curves be labelled $\mathbf{x}(z)$ and $\mathbf{y}(z)$. Also

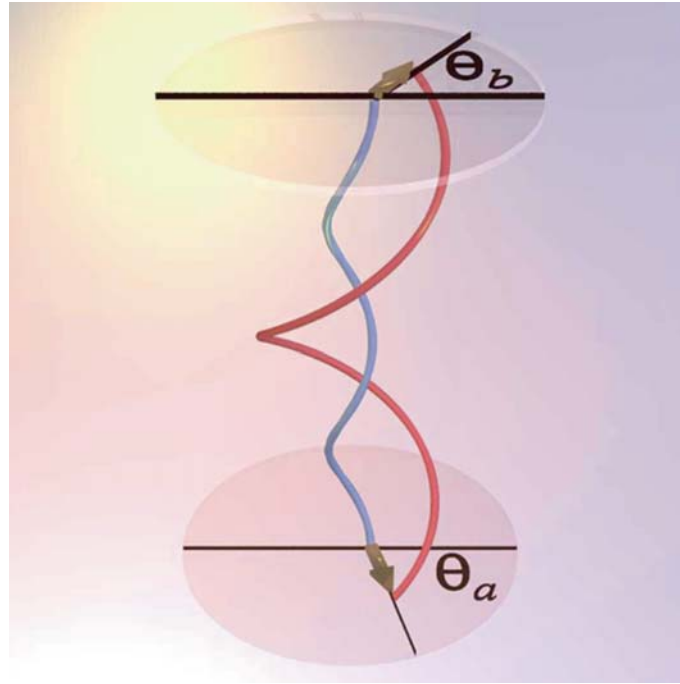


Fig. 2 Two braided curves \mathbf{x} and \mathbf{y} . Both curves have endpoints on horizontal planes $z = a$ and $z = b$. We assume both curves are oriented upwards, i.e. $dz/ds > 0$ where s denotes arclength. The horizontal axis is shown on both planes. Also, a relative position vector has been drawn on each plane between the endpoints of curve \mathbf{x} and curve \mathbf{y} . The angles between these vectors and the x axis are labelled Θ_a and Θ_b . For these curves, the net winding number is $w = 1 + (\Theta_b - \Theta_a)/2\pi$. The extra unit arises because the branch cut in angle has been crossed, in this case because the curves wrap by more than 2π .

let $\mathbf{r}(z) = \mathbf{y}(z) - \mathbf{x}(z)$ be the relative position vector pointing from \mathbf{x} to \mathbf{y} . This vector is horizontal; we will be interested in how much it rotates as it rises from the bottom to the top. Recall from elementary mechanics that the angular velocity $d\Theta/dt$ of a particle moving in the $x - y$ plane with position vector $\mathbf{r}(t)$ is given by

$$\frac{d\Theta}{dt} = \frac{(\mathbf{r} \times d\mathbf{r}/dt)_z}{r^2}. \quad (1)$$

Similarly the rotation rate of our two curves as they go upwards is

$$\frac{d\Theta}{dz} = \frac{(\mathbf{r} \times d\mathbf{r}/dz)_z}{r^2}. \quad (2)$$

Let $\Theta(z = a) = \Theta_a$ be the orientation of $\mathbf{r}(a)$ with respect to the x axis, i.e. $\mathbf{r}(a) = r_a(\cos \Theta_a, \sin \Theta_a)$. We place the discontinuity (branch cut) in Θ on the negative x axis, i.e. $-\pi < \Theta \leq \pi$. For the winding number, we count a complete turn as one unit, so the net winding is given by

$$w_{\mathbf{xy}} = \frac{1}{2\pi} \left(\int_a^z \frac{d\Theta}{dz'} dz' \right); \quad (3)$$

$$= \frac{1}{2\pi} (\Theta_b - \Theta_a) + n, \quad (4)$$

where n is an integer counting the number of times the angle rotates through the branch cut in the anti-clockwise direction.

Note that $w_{\mathbf{xy}}$ is independent of choice of x axis: a rotation of coordinates through $\delta\theta$ in the $x - y$ plane (or alternatively a uniform rotation of the braid through $-\delta\theta$ leaving the coordinates fixed) does not change $w_{\mathbf{xy}}$. To see this, first note that away from branch cuts, both Θ_b and Θ_a change by $\delta\theta$, so equation (4) stays fixed. Also, if (say) Θ_b crosses the cut at $\pm\pi$, then it will jump by $\pm 2\pi$, but n will jump at the same time by ∓ 1 .

In addition, $w_{\mathbf{xy}} = w_{\mathbf{yx}}$: reversing \mathbf{x} and \mathbf{y} adds $\pm\pi$ to both Θ_b and Θ_a without changing n .

Finally, we note that a computer may be more efficient at simply detecting crossings of the negative x axis than in directly integrating $d\Theta/dz$, so equation (4) may be faster than equation (3) in computing w .

2.2 General Curves

Next consider curves that travel both upwards and downwards; for example the two closed curves in figure 1. If we chop them into sections at their maxima and minima then we can ask about the winding number between each pair of sections. Figure 3 shows the two sections \mathbf{x}_2 and \mathbf{y}_2 . These sections overlap between z_{\min} and z_{\max} . Both sections travel downwards; i.e. $dz/ds < 0$ for both. Let σ denote the sign of dz/ds , and let

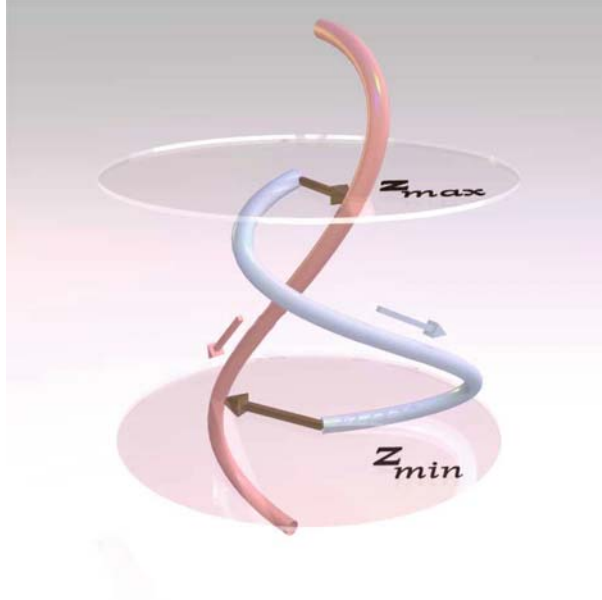


Fig. 3 The two sections x_2 and y_2 of the curves in figure 1. The relative position vectors are shown at the maximum and minimum heights z_{\max} , z_{\min} where these two sections overlap.

$$w_{22} = \frac{\sigma(\mathbf{x}_2)\sigma(\mathbf{y}_2)}{2\pi} \int_{z_{\min}}^{z_{\max}} \frac{d\Theta}{dz} dz. \quad (5)$$

Then for these curves

$$w_{22} = \frac{1}{2\pi} (\Theta_{\max} - \Theta_{\min}) \quad (6)$$

(for this diagram $\Theta(z)$ does not cross a branch cut, and so $n = 0$).

In the example shown in figure 4, curve 1 is monotonic, but curve 2 has a maximum at z_2 and a minimum at z_3 , so must be chopped into three pieces, $j = 1, 2, 3$. Let w_{ij} measure the net winding of piece i of curve 1 with piece j of curve 2. The first curve has just one piece, so we can write

$$w = w_{11} + w_{12} + w_{13} \quad (7)$$

where

$$w_{11} = \frac{1}{2\pi} \int_a^{z_2} \frac{d\Theta}{dz} dz; \quad w_{12} = -\frac{1}{2\pi} \int_{z_2}^{z_3} \frac{d\Theta}{dz} dz; \quad (8)$$

$$w_{13} = \frac{1}{2\pi} \int_{z_3}^b \frac{d\Theta}{dz} dz. \quad (9)$$

The integrals give

$$w_{11} = \frac{1}{2\pi}(\Theta(z_2) - \Theta_a) + n_{11}; \quad (10)$$

$$w_{12} = -\frac{1}{2\pi}(\Theta(z_2) - \Theta(z_3)) + n_{12}; \quad (11)$$

$$w_{13} = \frac{1}{2\pi}(\Theta_b - \Theta(z_3)) + n_{13}; \quad (12)$$

$$w = \frac{1}{2\pi}(\Theta_b - \Theta_a) + n_{11} + n_{12} + n_{13}. \quad (13)$$

Note that the intermediate angles $\Theta(z_2)$ and $\Theta(z_3)$ cancel out in the total winding number w .

We can now construct general expressions for the winding numbers between two arbitrary curves. For each section of a curve we define a function $\sigma(z)$ which first tells us whether the piece exists at z , and if so, then tells us whether it is rising or falling, i.e. gives the sign of dz/ds . In general, we will only consider curves with a finite set of discrete points where $dz/ds = 0$. Say curve α has n of pieces in between these turning points. Piece i starts at some height z_i and ends at height z_{i+1} . Define

$$\sigma_{\alpha i}(z) = \begin{cases} 1, & z \in (z_i, z_{i+1}) \text{ and } dz/ds > 0; \\ -1, & z \in (z_i, z_{i+1}) \text{ and } dz/ds < 0; \\ 0, & z \notin (z_i, z_{i+1}). \end{cases} \quad (14)$$

For example, the curves in figure 4 have winding number

$$w = \sum_{j=1}^3 w_{1j}; \quad w_{1j} = \sigma_1 \sigma_{2j} \frac{1}{2\pi} \int_a^b \frac{d\Theta}{dz} dz. \quad (15)$$

Let us define a generalized winding number $w[a, b]$ measuring the rotation of two curves between heights $z = a$ and $z = b$: if the curves can be cut into m_1 and m_2 pieces, then

$$w[a, b] = \sum_{i=1}^{m_1} \sum_{j=1}^{m_2} w_{ij}[a, b]; \quad w_{ij}[a, b] = \sigma_{1i} \sigma_{2j} \frac{1}{2\pi} \int_a^b \frac{d\Theta_{ij}}{dz} dz. \quad (16)$$

Furthermore, if pieces $1i$ and $2j$ overlap between heights $z_{\min}(1i, 2j)$ and $z_{\max}(1i, 2j)$, and we let $\Theta_{ij \min}$ and $\Theta_{ij \max}$ be the orientations of the relative position vectors at these heights, then

$$w_{ij}[a, b] = \sigma_{1i} \sigma_{2j} \left(\frac{1}{2\pi} (\Theta_{ij \max} - \Theta_{ij \min}) + n_{ij} \right). \quad (17)$$

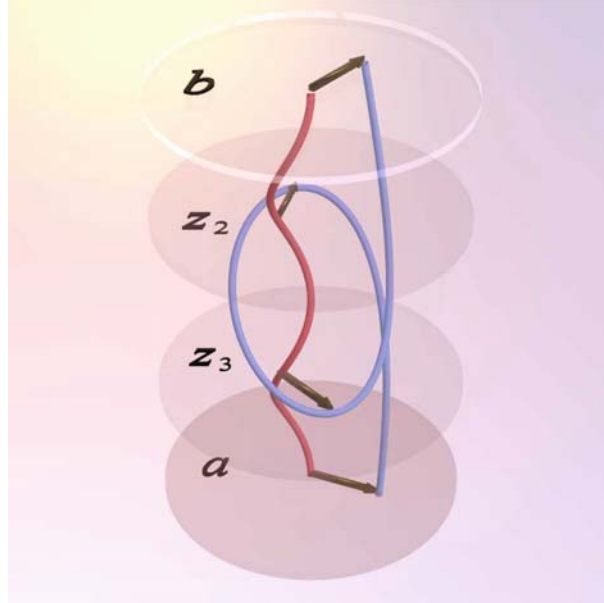


Fig. 4 Two tangled curves. The curve on the right starts at $z = a$, rises to a local maximum at $z = z_2$, wraps around the second curve as it descends to a local minimum at $z = z_3$, then rises to $z = b$. We will chop this curve at heights z_2 and z_3 . The relative position vectors $\mathbf{r}(z)$ are shown at $z_1 = a$, z_2 , z_3 , and $z_4 = b$. For these curves the total winding number is $w = 1 + (\Theta_b - \Theta_a)/2\pi$. Note that w does not depend on the intermediate angles $\Theta(z_2)$ or $\Theta(z_3)$.

2.3 Topological Invariance

Consider two curves with fixed endpoints on boundary planes, as in figure 2 and figure 4. Suppose we distort the curves *between* the two planes. As the endpoints are fixed, the boundary angles Θ_a and Θ_b do not change. But w equals $(\Theta_a - \Theta_b)/2\pi$ plus an integer. So w can only change by integer amounts due to the motion of the curves. If the two curves are allowed to pass through each other, then w will indeed change by ± 1 during each pass-through.

We will require that the curves do not pass through the boundary planes except at the endpoints. To see why, suppose one of the curves forms a loop which rises through the top plane. This loop can then jump over the top endpoint of the other curve. If the loop is then brought back downwards the new configuration will have a change in the winding number of ± 1 .

If the two curves are not allowed to pass through each other or loop-over, then a discrete change in w is not possible. To see this, note that equation (16) expresses w as a sum of integrals involving $d\Theta/dz$ (see equation (2)). Now $d\Theta/dz$ includes $|\mathbf{r}|^{-2}$, which goes singular if the curves pass through each other. Thus it is not surprising that w can jump in this

situation. But with material strings, or simply the restriction that $|\mathbf{r}| > 0$ at all times, the integrals evolve continuously, and jumps are not possible. These considerations suggest the following theorem:

Theorem 2.1 (Invariance of Winding Numbers). . *Suppose two curves stretch between the planes $z = a$ and $z = b$, where each curve has endpoints on both planes. Then their winding number $w[a, b]$ is invariant to continuous deformations of the curves in the region $a < z < b$ where*

1. *the endpoints are fixed;*
2. *the curves cannot pass through the boundary plane (except at their endpoints); and*
3. *the curves do not pass through each other.*

3 Linking Numbers

3.1 Winding Number Derivation

Next let us calculate the net winding number for two closed curves. Suppose the curves overlap in height between z_{\min} and z_{\max} . Suppose we define the quantity

$$\mathcal{L}_k = w[-\infty, \infty] = w[z_{\min}, z_{\max}]. \quad (18)$$

This quantity will turn out to be the *linking* number between the two curves.

Suppose, for example, that each curve has only one maximum and one minimum, as in figure 5. Generically, the two maxima and minima are at different heights. We again consider the orientation angles Θ of the relative position vectors $\mathbf{r}(z)$. The net winding angle will depend on two orientation angles Θ_A, Θ_B at the lower of the two maxima, and two orientation angles Θ_C, Θ_D at the upper of the two minima. We have

$$w_{11} = \frac{1}{2\pi}(\Theta_A - \Theta_C) + n_{11}; \quad (19)$$

$$w_{12} = -\frac{1}{2\pi}(\Theta_B - \Theta_D) + n_{12}; \quad (20)$$

$$w_{21} = -\frac{1}{2\pi}(\Theta_A - \Theta_C) + n_{21}; \quad (21)$$

$$w_{22} = \frac{1}{2\pi}(\Theta_B - \Theta_D) + n_{22}; \quad (22)$$

$$W = \sum_{i,j=1}^2 w_{ij} = n_{11} + n_{12} + n_{21} + n_{22}. \quad (23)$$

All the principal angles cancel out, leaving us with an integer

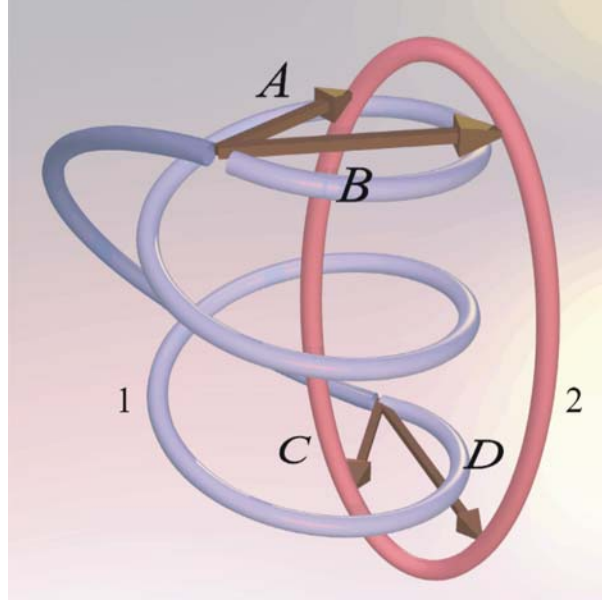


Fig. 5 Two closed curves. The relative position vectors \mathbf{r}_A , \mathbf{r}_B , \mathbf{r}_C , \mathbf{r}_D are shown at the maximum and minimum points on curve 1, $z_{1\max}$ and $z_{1\min}$.

$$\mathcal{L}_k = \sum_{i,j} n_{ij}. \quad (24)$$

The linking number is invariant to any distortion of the curves (without letting them pass through each other). First, an integer cannot continuously change to another integer! Only discrete changes are conceivable – for example, if the two curves do pass through each other then that would constitute a discrete event. Now, in the winding number calculation, the integer counts how many times the relative position angles $\Theta_{ij}(z)$ pass through the branch cut. One could rotate parts of the curves to remove any particular branch cut pass – however, another branch pass will just be created elsewhere. This is because the relative position angle must change through a whole range of 2π to increase the winding number by $+1$.

3.2 General Properties

Let the tangent vector to a curve \mathbf{x} (parametrized by arclength s) be defined by

$$\hat{\mathbf{T}}(s) = \frac{d\mathbf{x}}{ds}. \quad (25)$$

A tangent vector to a curve parameterized by arclength has unit norm, so $|\hat{\mathbf{T}}(s)| = 1$.

The Gauss linking number was originally defined as a double integral over two closed curves \mathbf{x} (with points $\mathbf{x}(s)$ and tangent $\mathbf{T}_{\mathbf{x}}(s)$) and \mathbf{y} (with points labelled $\mathbf{y}(s')$ and tangent $\mathbf{T}_{\mathbf{y}}(s')$):

$$\mathcal{L}_k \equiv \frac{1}{4\pi} \oint_{\mathbf{x}} \oint_{\mathbf{y}} \mathbf{T}_{\mathbf{x}}(s) \times \mathbf{T}_{\mathbf{y}}(s') \cdot \frac{\mathbf{x}(s) - \mathbf{y}(s')}{|\mathbf{x}(s) - \mathbf{y}(s')|^3} ds ds'. \quad (26)$$

In addition to being an integer and a topological invariant, linking number possesses the following properties:

1. \mathcal{L}_k equals half the signed number of crossings of the two curves as seen in any plane projection (see figure 5).
2. \mathcal{L}_k changes to $-\mathcal{L}_k$ if one of the curves changes direction ($\hat{\mathbf{T}} \rightarrow -\hat{\mathbf{T}}$). It thus is invariant to a change in direction of both curves.

4 Twist and Writhe Numbers

4.1 Ribbons

Suppose we compute the linking number of two curves which closely track each other. We will call one of the curves the *axis curve* \mathbf{x} ; the other will be the *secondary curve* \mathbf{y} . For example, the two curves might be the bounding curves of a ribbon, or the central axis and one of the two strands of a DNA double helix.

Suppose we parameterize the axis by some variable t (popular choices might be $t = z$, vertical height, or $t = s$, arclength); then we will let $\hat{\mathbf{V}}(t)$ be a unit vector normal to $\hat{\mathbf{T}}(t)$ pointing towards $\mathbf{y}(t)$. In particular,

$$0 = \hat{\mathbf{V}}(t) \cdot \hat{\mathbf{T}}(t); \quad (27)$$

$$\mathbf{y}(t) = \mathbf{x}(t) + \epsilon(t)\hat{\mathbf{V}}(t). \quad (28)$$

Here we will assume that the distance $\epsilon(t)$ between the two curves is small; for example smaller than the radius of curvature of $\mathbf{x}(t)$. Note that, while we can parameterize both curves by $t = s$, the parameter s measures arclength along the axis curve, not along the secondary curve.

The Gauss linking integral, equation (26), can be computed as usual. But note the term in the denominator. If we let $\epsilon \rightarrow 0$, so that the two curves coincide, then this denominator can vanish for the set of points $s = s'$. As this is only a one-dimensional subset of the two dimensional set of points s, s' , the singularity is not fatal. Călugăreanu [C59] studied this limit in detail, and showed that the linking number (at finite but small ϵ) can be decomposed

into two terms:

$$\mathcal{L}_k = \mathcal{W}_r + \mathcal{T}_w. \quad (29)$$

Here the *writhe* number \mathcal{W}_r is the limiting integral (when both line integrals go along the axis curve),

$$\mathcal{W}_r \equiv \frac{1}{4\pi} \oint_{\mathbf{x}} \oint_{\mathbf{x}} \hat{\mathbf{T}}(s) \times \hat{\mathbf{T}}(s') \cdot \frac{\mathbf{x}(s) - \mathbf{x}(s')}{|\mathbf{x}(s) - \mathbf{x}(s')|^3} ds ds', \quad (30)$$

while the *twist* number \mathcal{T}_w is defined by

$$\mathcal{T}_w \equiv \frac{1}{2\pi} \oint_{\mathbf{x}} \hat{\mathbf{T}}(s) \cdot \hat{\mathbf{V}}(s) \times \frac{d\hat{\mathbf{V}}(s)}{ds} ds \quad (31)$$

$$= \frac{1}{2\pi} \oint_{\mathbf{x}} \frac{1}{|\mathbf{v}(s)|^2} \hat{\mathbf{T}}(s) \cdot \mathbf{v}(s) \times \frac{d\mathbf{v}(s)}{ds} ds \quad (32)$$

where $\mathbf{v} = \epsilon \hat{\mathbf{V}}$.

Subsequent research has illuminated the meaning and properties of these two new quantities (see e.g. [F78, MR92, AKT95, C05]). As a quick (but not always accurate) guide, the writhe of a curve measures how much it kinks and coils, while twist measures how much a secondary curve twists about the first. The main application of these terms has been to DNA studies [VM97]. A DNA molecule has two strands which wind about each other thousands of times. Some of the winding number (or linking number if the DNA is closed) arises from local twist of the strands about the axis of the molecule, and the remainder arises because of coiling of the axis itself. As DNA can be centimetres long if fully stretched out, it needs a great deal of coiling to fit into a microscopic cell!

Twist has some special properties:

1. First, linking number and writhe are double integrals – while \mathcal{T}_w is a single integral. Thus it is meaningful to write twist as the sum of a local density along the curve:

$$\mathcal{T}_w = \frac{1}{2\pi} \oint_{\mathbf{x}} \frac{d\mathcal{T}_w}{ds} ds. \quad (33)$$

2. $d\mathcal{T}_w/ds$ measures the rotation rate of the secondary curve about the axis curve, in the plane perpendicular to the tangent vector $\mathbf{T}_{\mathbf{x}}(s)$. Recall that equation (2) gives the angular velocity of a curve about the constant z direction. If instead we wished to find the angular velocity about the tangent direction, we would calculate

$$\frac{d\mathcal{T}_w}{ds} = \frac{1}{2\pi} \hat{\mathbf{T}}(s) \cdot \hat{\mathbf{V}}(s) \times \frac{d\hat{\mathbf{V}}(s)}{ds}. \quad (34)$$

3. We can calculate twist numbers for two neighboring magnetic field lines. Single out one field line and call it the ‘axis’; neighboring field lines are almost parallel to this axis line but may spiral about it. Let $\mathbf{J} = \wedge \mathbf{B}/\mu_0$ be the electric current associated with the magnetic field \mathbf{B} , and $J_{\parallel} = \mathbf{J} \cdot \mathbf{B}/|\mathbf{B}|$. Then by Stokes’ theorem applied to a small disc of radius r placed perpendicular to \mathbf{B} on the axis,

$$\mu_0 \pi r^2 J_{\parallel} = 2\pi r B_{\phi}, \quad (35)$$

where B_{ϕ} is the azimuthal field component generated by the parallel current. The parallel magnetic field is B_s , which equals $|\mathbf{B}|$ on the axis. In a local cylindrical coordinate system (r, ϕ, s) surrounding the axis field line, we can ask how far a neighboring field line travels in both the ϕ and s directions. The field line equations relate this travel to the components of the field vector:

$$\frac{B_{\phi}}{B_s} = \frac{r \delta \phi}{\delta s}. \quad (36)$$

Putting these equations together gives

$$\frac{d\mathcal{T}_w}{ds} = \frac{1}{2\pi} \frac{d\phi}{ds} = \frac{\mu_0 J_{\parallel}}{4\pi |\mathbf{B}|}. \quad (37)$$

Similarly, if we measure how much two neighboring flow lines in a fluid twist about each other, then

$$\frac{d\mathcal{T}_w}{ds} = \frac{\omega_{\parallel}}{4\pi |\mathbf{V}|}, \quad (38)$$

where \mathbf{V} is the fluid velocity and ω is the vorticity.

4. \mathcal{T}_w is independent of the direction of the axis curve. This is because the neighboring curves must be almost aligned with the axis, so flipping the direction of the axis also flips the neighbors.
5. \mathcal{T}_w equals half the average number of crossings between the two neighboring curves seen in projections of the curve onto a plane. The average is over all possible projection angles, and takes into account the sign of the crossing. Only local crossings are included in this average (if the axis curve crosses over some distant part of the secondary, this contributes to the writhe rather than the twist) [DH05].

Writhe also has some special properties:

1. Writhe depends on the axis curve only – the secondary curve is not needed for its definition.
2. Writhe equals the average number of crossings seen in projections of the curve. The average is over all possible projection angles [O94, DH05].
3. Writhe is independent of the direction of the axis curve.

4.2 Twisted Tubes

In many applications the picture of two curves twisting about each other is best replaced by thin tubes filled with curves. For example, vortex tubes and magnetic flux tubes play important roles in fluid mechanics and magnetohydrodynamics. In engineering and material science, *isotropic rods* [VT00] are twisted tubes with some elastic energy function that is independent of positions in cross-sections of the tube. To obtain a twisted tube from an axis curve $\mathbf{x}(t)$, we first draw a circle around the axis at each position t . These circles should be of constant radius ϵ , and perpendicular to the axis (i.e. perpendicular to $\hat{\mathbf{T}}(t)$). Joining up all the circles creates a tube enclosing the axis curve. We choose ϵ small enough so that the tube does not intersect itself.

Next we fill the tube with curves. These curves will be almost parallel to the axis, but may twist about the axis. We would like this twist to be uniform across a cross-section of the tube (but not necessarily uniform along the tube). Choose one of the curves and treat it like the secondary curve \mathbf{y} . The tube surface can be given coordinates (t, ϕ) with $\phi = 0$ on \mathbf{y} , so $\mathbf{y}(t)$ has coordinates $(t, 0)$. Let $\hat{\mathbf{W}} = \hat{\mathbf{T}} \times \hat{\mathbf{V}}$. Other curves (label them by the variable β) have different values of ϕ . Thus, on the surface (at radius ϵ)

$$\mathbf{y}(t, \beta) = \mathbf{x}(t) + \epsilon \left(\cos \beta \hat{\mathbf{V}}(t) + \sin \beta \hat{\mathbf{W}}(t) \right). \quad (39)$$

We can take the same tube with the same axis and fill it with many different sets of twisted curves. Each set, together with a particular choice of reference curve \mathbf{y} , defines a coordinate system in the tube. This coordinate system is called a *framing*. Some quantities, like the twist number between a secondary curve on the tube and the axis, explicitly depend on the choice of framing. Other quantities, like the writhe, depend only on the axis curve so are independent of framing.

We will sometimes need to take averages over all secondary curves. Given a number $f(\beta)$ describing the geometry of one of the secondary curves, let

$$\langle f \rangle \equiv \frac{1}{2\pi} \int_0^{2\pi} f(\beta) d\beta. \quad (40)$$

5 Writhe from Winding Numbers

We can use the winding number techniques from sections 2 and 3 to simplify the calculation of writhe. These techniques will also help in extending the definition of writhe to open curves; in particular curves with endpoints on boundary planes (or spheres). Applications include isotropic rods fixed

between two planes [S05, RM03] and magnetic arches in the solar atmosphere [TK05]. For full details of the calculations below, see [BP06].

Define the linking number $\tilde{\mathcal{L}}(z_0)$ to be the net winding number between two curves between $z = -\infty$ and $z = z_0$. (One can replace $z = -\infty$ by z_{\min} , where z_{\min} is the minimum height at which the two curves are both present.) Then the total linking number will be

$$\mathcal{L}_k = \tilde{\mathcal{L}}(+\infty) = \tilde{\mathcal{L}}(z_{\max}). \quad (41)$$

Also define $\tilde{\mathcal{T}}(z_0)$ and $\tilde{\mathcal{W}}(z_0)$, the twist and writhe below z_0 , in the same manner. We can then take derivatives in the z direction and ask how these quantities grow with height. We will see below that all secondary curves on a tube have the same growth in twist relative to the axis, i.e. $d\tilde{\mathcal{T}}/dz$ is independent of β . For linking number we need to be more careful; we will need to average over β .

Suppose we reorder the Călugăreanu formula as $\mathcal{W}_r = \mathcal{L}_k - \mathcal{T}_w$. We can then take this formula as a *definition* of writhe, rather deducing it from the standard definition equation (30). But first we must make sure that this formula makes sense, i.e. that it always gives the same answer for the axis curve, no matter which framing is used. For the differential writhe this vital property will be achieved below by averaging over β ; thus we define

$$\frac{d\tilde{\mathcal{W}}}{dz} \equiv \left\langle \frac{d\tilde{\mathcal{L}}}{dz} - \frac{d\tilde{\mathcal{T}}}{dz} \right\rangle. \quad (42)$$

To simplify the equations, we denote derivatives in z by a prime. Suppose the axis curve \mathbf{x} has m intersections with the plane $z = \text{constant}$; in other words m segments of the axis curve exist at height z . Each of these segments \mathbf{x}_i has its corresponding secondary curve \mathbf{y}_i .

The linking number $\tilde{\mathcal{L}}$ sums winding numbers over all pairs of segments \mathbf{x}_i and \mathbf{y}_j . The axis curve segment \mathbf{x}_i has secondary \mathbf{y}_i ; if these wind about each other, they will contribute a *local* term

$$\tilde{\mathcal{L}}_i = w_{ii} = w(\mathbf{x}_i, \mathbf{y}_i) \quad (43)$$

to the total linking number. In addition, axis segment i winds about far away secondary segments \mathbf{y}_j , $j \neq i$. These windings contribute *nonlocal* terms

$$\tilde{\mathcal{L}}_{ij} \equiv \tilde{\mathcal{L}}(\mathbf{x}_i, \mathbf{y}_j) \equiv w(\mathbf{x}_i, \mathbf{y}_j). \quad (44)$$

In sum, the z derivative decomposes into local (diagonal) terms, and nonlocal (off-diagonal) terms:

$$\tilde{\mathcal{L}}'(z) = \sum_{i=1}^n \tilde{\mathcal{L}}'_i(z) + \sum_{i=1}^n \sum_{\substack{j=1 \\ i \neq j}}^n \tilde{\mathcal{L}}'_{ij}. \quad (45)$$

The following quantities will be useful:

$$\lambda = \frac{dz}{ds} = T_z; \quad (46)$$

$$\mu = |\hat{\mathbf{z}} \times \hat{\mathbf{T}}| = \sqrt{1 - \lambda^2}. \quad (47)$$

5.1 The Twist as a Function of Height

For the moment, consider a segment (labelled i) of the axis curve which travels upwards, so that $\lambda > 0$. From equation (34) (modified considering equation (39)), the z derivative of the twist is

$$\tilde{\mathcal{T}}_i'(z) = \frac{d\tilde{\mathcal{T}}_i(z)}{dz} = \frac{d\mathcal{T}_{wi}}{ds} \frac{ds}{dz} \quad (48)$$

$$= \frac{1}{2\pi} \hat{\mathbf{T}} \cdot \left(\cos \beta \hat{\mathbf{V}} + \sin \beta \hat{\mathbf{W}} \right) \times \left(\cos \beta \hat{\mathbf{V}}' + \sin \beta \hat{\mathbf{W}}' \right). \quad (49)$$

Because $\hat{\mathbf{V}}$ and $\hat{\mathbf{W}}$ are unit vectors $\hat{\mathbf{V}} \cdot \hat{\mathbf{V}}' = \hat{\mathbf{W}} \cdot \hat{\mathbf{W}}' = 0$. Also, $\hat{\mathbf{V}} \cdot \hat{\mathbf{W}} = 0$ so

$$\hat{\mathbf{W}} \cdot \hat{\mathbf{V}}' = -\hat{\mathbf{V}} \cdot \hat{\mathbf{W}}' \equiv \omega. \quad (50)$$

Thus

$$2\pi \tilde{\mathcal{T}}_i' = (\cos \beta \hat{\mathbf{W}} - \sin \beta \hat{\mathbf{V}}) \cdot (\cos \beta \hat{\mathbf{V}}' + \sin \beta \hat{\mathbf{W}}') \quad (51)$$

$$= \omega. \quad (52)$$

The twist $\tilde{\mathcal{T}}_i'$ is the same for all of the twisted curves on the surface of the tube, i.e. independent of β . However, ω does depend on the vectors $\hat{\mathbf{V}}(z)$ and $\hat{\mathbf{W}}(z)$. As we will see, this dependence on the framing will be cancelled when $\tilde{\mathcal{T}}'$ is subtracted from $\tilde{\mathcal{L}}'$ (averaged over β).

It will be convenient to define a new orthonormal frame:

$$\{\hat{\mathbf{T}}, \hat{\mathbf{f}}, \hat{\mathbf{g}}\} = \left\{ \hat{\mathbf{T}}, \frac{\hat{\mathbf{z}} \times \hat{\mathbf{T}}}{\mu}, \hat{\mathbf{T}} \times \frac{\hat{\mathbf{z}} \times \hat{\mathbf{T}}}{\mu} \right\}. \quad (53)$$

We can write $\hat{\mathbf{V}}$ and $\hat{\mathbf{W}}$ as combinations of $\hat{\mathbf{f}}$ and $\hat{\mathbf{g}}$ in terms of some angle $\psi(z)$:

$$\begin{pmatrix} \hat{\mathbf{V}} \\ \hat{\mathbf{W}} \end{pmatrix} = \begin{pmatrix} \cos \psi(z) & \sin \psi(z) \\ -\sin \psi(z) & \cos \psi(z) \end{pmatrix} \begin{pmatrix} \hat{\mathbf{f}} \\ \hat{\mathbf{g}} \end{pmatrix}. \quad (54)$$

The curve at position β is offset from the axis curve by

$$\hat{\mathbf{U}} = \left(\cos \beta \hat{\mathbf{V}} + \sin \beta \hat{\mathbf{W}} \right) = \cos(\beta + \psi) \hat{\mathbf{f}} + \sin(\beta + \psi) \hat{\mathbf{g}}. \quad (55)$$

In terms of ψ one finds

$$2\pi\tilde{\mathcal{T}}' = \omega = (\psi' + \hat{\mathbf{f}}' \cdot \hat{\mathbf{g}}) \quad (56)$$

$$= \psi' + \frac{\lambda}{\mu^2} \hat{\mathbf{z}} \cdot \hat{\mathbf{T}} \times \hat{\mathbf{T}}'. \quad (57)$$

5.2 The Local Winding Number as a Function of Height

We now calculate the local winding between the axis and the secondary, as in equation (43):

$$\tilde{\mathcal{L}}'_i(z) = w'(\mathbf{x}_i(z), \mathbf{y}_i(z)) = \frac{1}{2\pi} \Theta'(\mathbf{x}_i(z), \mathbf{y}_i(z)). \quad (58)$$

Here we run into a difficulty: the point on the secondary curve $\mathbf{y}_i(z)$ corresponds to a different arclength parameter s than the axis point $\mathbf{x}_i(z)$. In fact, to first order in ϵ (Berger & Prior 2006)

$$\mathbf{y}_i(z) - \mathbf{x}_i(z) = \epsilon \left(\hat{\mathbf{U}} - \lambda^{-1} U_z \hat{\mathbf{T}} \right). \quad (59)$$

Let $\mathbf{R}_i = (\mathbf{y}_i - \mathbf{x}_i)/\epsilon$. From equation (2),

$$2\pi\tilde{\mathcal{L}}'_i(z) = \frac{\hat{\mathbf{z}} \cdot \mathbf{R}_i(z) \times \mathbf{R}'_i(z)}{|\mathbf{R}_i(z)|^2}. \quad (60)$$

After some algebra,

$$\frac{\hat{\mathbf{z}} \cdot \mathbf{R}_i \times \mathbf{R}'_i}{\mathbf{R}_i^2} = \frac{\lambda\psi' - \lambda' \cos(\beta + \psi) \sin(\beta + \psi)}{(\lambda^2 \cos^2(\beta + \psi) + \sin^2(\beta + \psi))} + \frac{1}{\mu^2} \hat{\mathbf{z}} \cdot \hat{\mathbf{T}} \times \hat{\mathbf{T}}'. \quad (61)$$

This messy expression simplifies considerably if we average over all secondary curves in the tube:

$$2\pi\langle\tilde{\mathcal{L}}'_i\rangle = \frac{1}{2\pi} \int_0^{2\pi} \frac{\hat{\mathbf{z}} \cdot \mathbf{R}_i \times \mathbf{R}'_i}{\mathbf{R}_i^2} d\beta \quad (62)$$

$$= \psi' + \frac{1}{\mu^2} \hat{\mathbf{z}} \cdot \hat{\mathbf{T}} \times \hat{\mathbf{T}}'. \quad (63)$$

5.3 The Local Writhe as a Function of Height

We now, in effect, subtract section 5.1 from section 5.2. This will give us the local part of the writhe of segment i . From equation (57) and equation (63),

$$\widetilde{\mathcal{W}}'_i \equiv \langle \widetilde{\mathcal{L}}'_i - \widetilde{\mathcal{T}}'_i \rangle \quad (64)$$

$$= \frac{1-\lambda}{\mu^2} \hat{\mathbf{z}} \cdot \hat{\mathbf{T}} \times \hat{\mathbf{T}}'. \quad (\lambda > 0). \quad (65)$$

So far we have assumed $\lambda = dz/ds > 0$ on segment i . We can obtain the result for negative λ most simply by noting that if we reverse arclength, i.e. let $s \rightarrow -s$, then linking, twist, and writhe do not change. Meanwhile, $\hat{\mathbf{T}} \rightarrow -\hat{\mathbf{T}}$ and $\hat{\mathbf{T}}' \rightarrow -\hat{\mathbf{T}}'$. Thus to preserve the value of $\widetilde{\mathcal{W}}'_i$, λ must be replaced by $|\lambda|$:

$$\widetilde{\mathcal{W}}'_i = \frac{1-|\lambda|}{\mu^2} \hat{\mathbf{z}} \cdot \hat{\mathbf{T}} \times \hat{\mathbf{T}}'. \quad (66)$$

(As an exercise, one may compute $\widetilde{\mathcal{W}}'_i$ directly for negative λ . Some of the relations in the calculation above need amendment; for example if s_{\max} is the maximum s value on the segment, then write $\widetilde{\mathcal{T}}(z) = \mathcal{T}_w(s_{\max}) - \mathcal{T}_w(s(z))$. Also one must replace ψ by $\pi - \psi$.)

5.4 The Nonlocal Winding Number as a Function of Height

From equation (44), for $i \neq j$

$$\widetilde{\mathcal{L}}'_{ij}(z) = w'(\mathbf{x}_i(z), \mathbf{y}_j(z)). \quad (67)$$

But the distance between $\mathbf{x}_i(z)$ and $\mathbf{y}_j(z)$ is much greater than that between $\mathbf{x}_j(z)$ and $\mathbf{y}_j(z)$, so (strictly speaking, in the limit $\epsilon \rightarrow 0$)

$$\widetilde{\mathcal{L}}'_{ij}(z) = w'(\mathbf{x}_i(z), \mathbf{x}_j(z)) = \frac{1}{2\pi} \sigma_i \sigma_j \Theta'(\mathbf{x}_i(z), \mathbf{x}_j(z)) \quad (i \neq j). \quad (68)$$

Thus the $m(m-1)$ off-diagonal terms in equation (45) depend only on the axis curve. These represent non-local windings of the different segments of the axis curve about each other.

We can now write down the entire expression for the writhe [BP06]:

Theorem 5.1.

$$\mathcal{W}_r = \widetilde{\mathcal{W}}_{local} + \widetilde{\mathcal{W}}_{nonlocal}; \quad (69)$$

$$\widetilde{\mathcal{W}}_{local} = \frac{1}{2\pi} \sum_{i=1}^n \int_{z_i^{\min}}^{z_i^{\max}} \frac{1}{(1 + |\lambda_i|)} (\hat{\mathbf{T}}_i \times \hat{\mathbf{T}}'_i)_z dz; \quad (70)$$

$$\widetilde{\mathcal{W}}_{nonlocal} = \sum_{i=1}^n \sum_{\substack{j=1 \\ i \neq j}}^n \frac{\sigma_i \sigma_j}{2\pi} \int_{z_{ij}^{\min}}^{z_{ij}^{\max}} \Theta'_{ij}(z) dz. \quad (71)$$

In terms of the intrinsic quantities *curvature* κ and *binormal* $\hat{\mathbf{B}}$,

$$(\hat{\mathbf{T}}_i \times \hat{\mathbf{T}}'_i)_z = \frac{\kappa_i B_{zi}}{\lambda_i}. \quad (72)$$

Note that the nonlocal writhe involves integrals of θ'_{ij} . We can treat these the same way as winding numbers, equation (17). In contrast to the linking number calculation, however, not all of the angles cancel. One finds that the orientations of the tangent vectors at the maxima and minima contribute to the sums. In particular, if $\phi(z_i^{\min})$ and $\phi(z_i^{\max})$ are the angles with respect to the x axis of the tangent vectors $\hat{\mathbf{T}}(z_i^{\min})$ and $\hat{\mathbf{T}}(z_i^{\max})$, then

$$\widetilde{\mathcal{W}}_{nonlocal} = \frac{1}{2\pi} \sum_{i=1}^n (\phi(z_i^{\min}) - \phi(z_i^{\max})) - 1 + \sum_{i=1}^n \sum_{\substack{j=1 \\ i \neq j}}^n \sigma_i \sigma_j n_{ij}. \quad (73)$$

Thus we do not need to perform the integrals completely – although we still need to keep track of the branch crossings to calculate the n_{ij} terms.

5.5 Example: A Trefoil Torus Knot

Figure 6 shows a trefoil knot. It is constructed by following a curve imbedded in a torus, which winds three times the short way around and two times the long way around. The 3 maxima and 3 minima in z divide the curve into 6 segments. For this curve the net local writhe of the 6 segments is -0.71 , the nonlocal writhe between all pairs of segments sums to 4.23 , giving a total writhe of $\mathcal{W}_r = 3.52$. Figure 7 displays a different version of the trefoil, a $(3,2)$ torus knot; this curve has a higher writhe [MR92].

The trefoil figures also show the associated *tantrix curves*. As a tangent vector is defined to have unit norm, its tip lives on a unit sphere. As we go around the knot, the tip of the tangent vector traces this curve on the *tantrix sphere*.

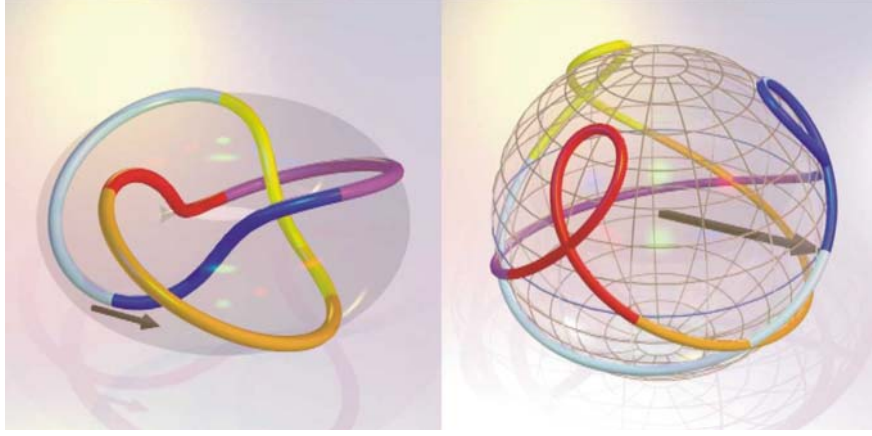


Fig. 6 The left figure displays a torus, with a ratio of major axis to minor axis equal to 2. A curve winds about this torus, forming a (2,3) torus knot, which is classified as a trefoil knot. The arrow shows the tangent vector at one point on the knot. Tangent vectors have unit norm, so if we place them inside a unit sphere, their tips just touch the surface. The figure on the right shows a unit sphere, called the *tantrix sphere*. The arrow touching this sphere represents the same tangent vector illustrated on the knot. The curve shown on the sphere gives the direction of the tangent vector at every point on the knot.

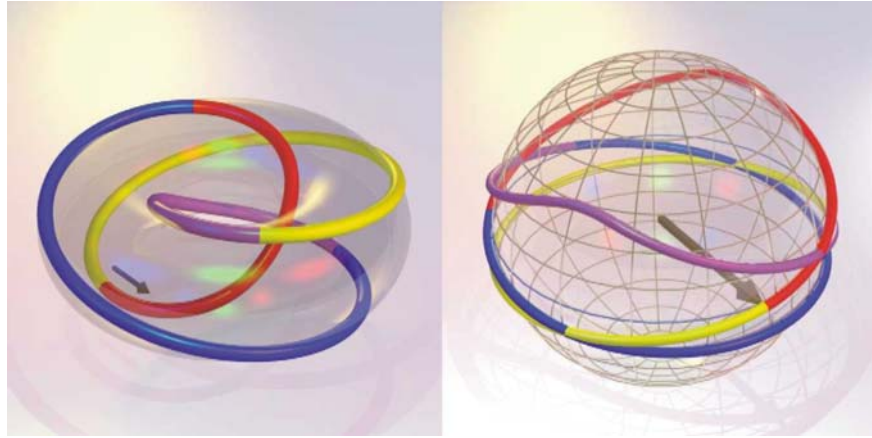


Fig. 7 As in figure 6, but with a (3,2) torus knot. For this curve, the local writhe is -0.51, the nonlocal writhe is 4.41, with a total writhe $\mathcal{W}_r = 3.90$.

Recall that the knot is divided at extrema, where $T_z = dz/ds = 0$; this implies that the tantrix curve crosses the equator of the tantrix sphere at these points. The local writhe for each segment equals the area between the corresponding tantrix segment and the North pole (if the segment is in the Northern hemisphere) or the South pole (if in the Southern hemisphere).

(The area enclosed by a curve drawn on a sphere is considered positive if the curve rotates anti-clockwise about the region and negative if clockwise.)

To see this, note that if θ gives latitude on the tantrix sphere, then $\lambda = \cos \theta$ and $\mu = \sin \theta$. Also,

$$\widehat{\mathbf{T}}' dz = d\widehat{\mathbf{T}} = d\theta \hat{\theta} + \sin \theta d\phi \hat{\phi}. \quad (74)$$

With $\hat{z} \times \widehat{\mathbf{T}} = \sin \theta \hat{\phi}$ we can write

$$(\widehat{\mathbf{T}} \times \widehat{\mathbf{T}}') \cdot \hat{z} dz = \sin^2 \theta d\phi, \quad (75)$$

and so

$$2\pi \widetilde{\mathcal{W}}'_{local}(z) = \frac{1}{(1 + |\cos \theta|)} \sin^2 \theta \frac{d\phi}{dz} \quad (76)$$

$$= (1 - |\cos \theta|) \frac{d\phi}{dz}. \quad (77)$$

Integrating between z_0 and z_1 gives

$$\widetilde{\mathcal{W}}_{local}(z_0, z_1) = \frac{1}{2\pi} \int_{z_0}^{z_1} (1 - |\cos \theta|) \frac{d\phi}{dz} dz. \quad (78)$$

For Northern segments with $d\phi/dz$ positive this gives the area swept out between the tantrix and the North pole. For Southern segments, $d\phi/dz$ positive implies clockwise (negative) winding about the South pole. Thus $\widetilde{\mathcal{W}}_{local}(z_0, z_1)$ gives the negative of the area below the tantrix for Southern segments.

6 Writhe for Open Curves

The winding number techniques described here can be used to measure the writhe of open curves. Consider a curve confined between two parallel boundary planes at $z = a$ and $z = b$, with endpoints on the planes, as in equation (2). We can then define the writhe of this curve simply as the integral from a to b of $\widetilde{\mathcal{W}}'(z)$. This quantity is called the *polar writhe* in [BP06], as it is related to the area between the tantrix curve and the pole, as described in the previous section. Several other definitions appropriate for open writhe have appeared in the literature; these have usually involved considering perturbations of a reference curve [F78, AKT95, RM03] or closing the curve in a suitable way [S05].

The polar writhe is also relevant for *loops*, here defined as a curve confined to one half-space, with endpoints on the boundary plane of the half-space. Instead of a half-space and boundary plane, we can also consider loops

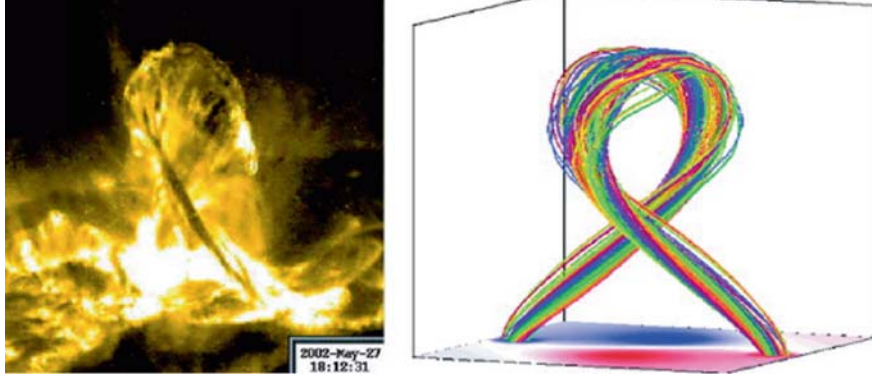


Fig. 8 A filament of hot plasma in the solar corona observed by the TRACE detector on 27 May 2002. The plasma is thought to follow the path of magnetic field lines. The right picture displays a numerical simulation of the associated magnetic field [TK05].

extending from a boundary sphere (this requires modifying planar angles into spherical angles in the winding number calculations). Loops are of considerable importance in astrophysics, as magnetic field lines often form loops in the atmospheres of stars and accretion disks. Figure 8 shows one example from solar observations. Loops of magnetic flux often acquire a significant amount of twist; kink instabilities can convert some of this twist to writhe [LK97, Ba00, R05]).

The polar writhe is consistent with magnetic helicity integrals over volumes bounded by planes or spheres [BP06]). In particular, we can decompose the helicity of a magnetic flux loop of flux Φ as

$$H = (\mathcal{T}_w + \widetilde{\mathcal{W}})\Phi^2. \quad (79)$$

Figure 9 shows two loops; both were generated by taking an inverted parabola and twisting the top. The loops look quite different and yet have the same writhe. We can interpret this result in terms of the balance between local and nonlocal writhe. The tall loop has positive $\widetilde{\mathcal{W}}_{local}$ and negative $\widetilde{\mathcal{W}}_{nonlocal}$. The same total can be reached with negative $\widetilde{\mathcal{W}}_{local}$ and positive $\widetilde{\mathcal{W}}_{nonlocal}$, but with a shorter height. This may have implications for the interpretation of observations of structures in the solar atmosphere. Soft x-ray emissions in the shape of an *S* shaped curve, called *sigmoids*, are often seen in solar observations [RK96]. *S* shapes appear preferentially in the Southern hemisphere, whereas inverse *S* (or *Z*) shapes appear preferentially in the North. The shape may depend on the sign of writhe for the structure. However, assigning the sign of $\widetilde{\mathcal{W}}$ to an *S* or *Z* shape may depend on the height of the structure.

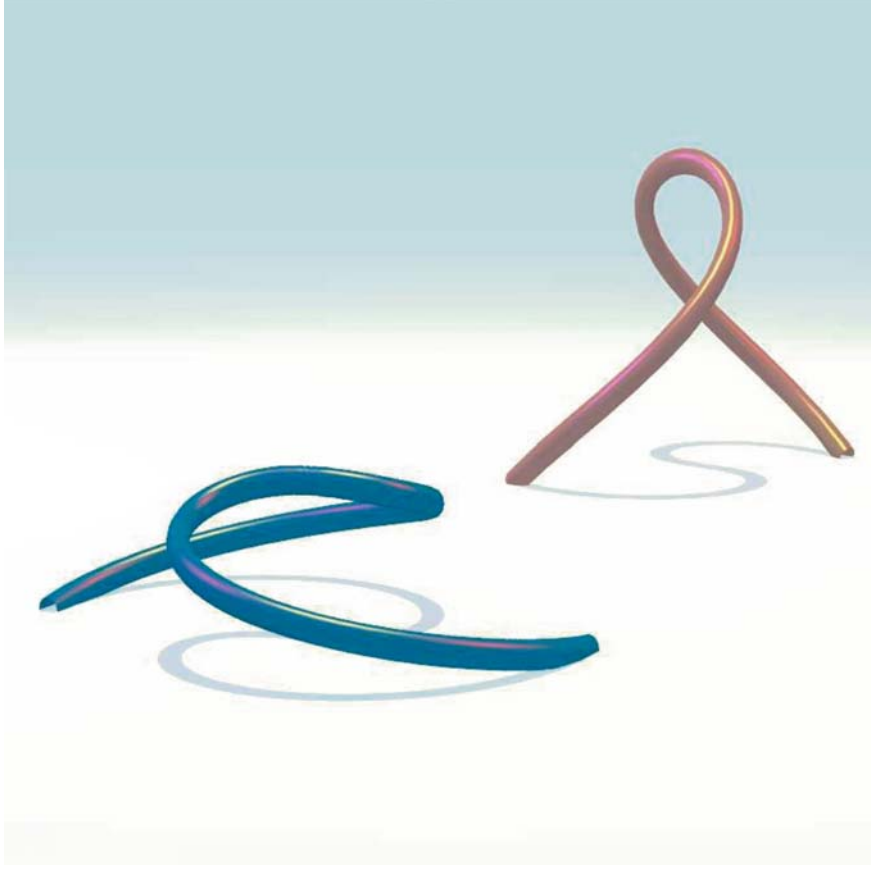


Fig. 9 Two loops. For the short loop on the left, $\mathcal{W}_{rlocal} = -1.2$, $\mathcal{W}_{rnonlocal} = 1$. For the tall loop on the right, $\mathcal{W}_{rlocal} = 0.466$, $\mathcal{W}_{rnonlocal} = -2/3$. Thus the signs of both local and nonlocal writhe are opposite for the two loops, yet they have the same total polar writhe $\mathcal{W}_r = -0.2$. This demonstrates how the writhe can depend on height as well as which direction the loop turns. Note that in projection the tall loop has an *S* shape, while the short loop has an inverse *S* shape.

7 Higher Order Winding

Winding and Linking numbers do not capture all of the topological properties of curves. Figure 10 shows two braids. In the first braid, the curves wind about each other, but in a simple way. In the second braid, no two curves have net winding number, and yet the curves intertwine in a more complex way. This intertwining can be captured by computing a *second order winding number* [B91].



Fig. 10 Two braids. The left braid only exhibits ordinary (first order) winding. The right figure shows a pigtail braid with second order winding.

Suppose we replace Cartesian coordinates (x, y, z) by a pair (c, z) where c is a complex number $c = x + iy$. Let $(c_1(z), z)$, $(c_2(z), z)$ be two curves. Let

$$\lambda_{12}(z) = \frac{1}{2\pi i} \int_{-\infty}^z \sigma_1 \sigma_2 \frac{d \ln (c_2(z') - c_1(z'))}{dz'} dz'. \quad (80)$$

Then the winding number is related to this complex logarithm, $w_{12}(z) = \text{Re } \lambda_{12}(z)$. Note that by defining λ_{12} as an integral of $d \ln(c_2 - c_1)/z$ rather than simply $\ln(c_2 - c_1)$, we allow winding numbers outside of the interval $(-1/2, 1/2)$.

Next, we can obtain second order winding numbers for three braided curves c_1, c_2, c_3 by integrating suitable combinations of the λ functions. Suppose the curves travel from $z = 0$ to $z = 1$. Then the second order winding number is

$$\Psi = \frac{1}{2} \int_0^1 ((\lambda_{12} - \lambda_{23}) d\lambda_{31} + (\lambda_{23} - \lambda_{31}) d\lambda_{12} + (\lambda_{31} - \lambda_{12}) d\lambda_{23}). \quad (81)$$

This quantity is invariant to deformations of the curves, leaving their end-points fixed. Third and higher order invariants for braids [B01] or knots and links [CD00] require the machinery of Kontsevich integrals [K93] to identify the appropriate combinations of λ functions.

References

- [AKT95] Aldinger J, Klapper I, & Tabor M: Formulae for the calculation and estimation of writhe. *J. Knot Theory Ram.*, **4**, 343–372 (1995)
- [B91] Berger M A: Third order braid invariants. *J. Physics A: Mathematical and General*, **24**, 4027–4036 (1991)

- [B01] Berger M A: Topological invariants in braid theory. *Letters in Math. Physics*, **55**, 181–192 (2001)
- [BP06] Berger M A & Prior P: The writhe of open and closed curves. *J. Physics A: Mathematical and General*, **39**, 8321–8348 (2006)
- [Ba00] Baty H: Magnetic topology during the reconnection process in a kinked coronal loop. *Astronomy and Astrophysics*, **360**, 345–350 (2000)
- [C59] Călugăreanu G: Sur les classes d’isotopie des noeuds tridimensionnels et leurs invariants. *Czechoslovak Math J*, **11**, 588–625 (1959)
- [C05] Cantarella J: On comparing the writhe of a smooth curve to the writhe of an inscribed polygon. *SIAM J. of Numerical Analysis*, **42**, 1846–1861 (2005)
- [CD00] Chmutov S V & Duzhin S V: The Kontsevich Integral. *Acta Appl. Math.*, **66**, 155–190 (2000)
- [DH05] Dennis M R & Hannay J H: Geometry of Călugăreanu’s theorem. *Proc. Roy. Soc. A*, **461**, 3245–3254 (2005)
- [F78] Fuller F B: Decomposition of the linking of a ribbon: a problem from molecular biology. *Proc. Natl. Acad. Sci. USA*, **75**, 3557–3561 (1978)
- [GVV03] Ghrist R W, Van den Berg J B, & Vandervorst R C: Morse theory on spaces of braids and Lagrangian dynamics. *Inventiones Mathematicae*, **152**, 369–432 (2003)
- [K93] Kontsevich M: Vassiliev’s knot invariants. *Adv. Soviet Math.*, **16**, 137–150 (1993)
- [KHS06] Kristiansen K D, Helgesen G, Skjeltorp A T: Braid theory and Zipf-Mandelbrot relation used in microparticle dynamics. *European Physical J.*, **B 51**, 363–371 (2006)
- [LK97] Longcope D W & Klapper I: Dynamics of a thin twisted flux tube. *Astrophysical J.*, **488**, 443–453 (1997)
- [MR92] Moffatt H K & Ricca R L: Helicity and the Călugăreanu invariant. *Proc. Roy. Soc. A*, **439**, 411–429 (1992)
- [O94] Orlandini E, Test M C, Whittington S G, Sumners D W, & Janse van Rensburg E J: The writhe of a self-avoiding walk. *J. Physics A: Mathematical and General*, **27**, L333–L338 (1994)
- [R05] Ricca R L: Inflexional disequilibrium of magnetic flux-tubes. *Fluid Dynamics Research*, **36**, 319–332 (2005)
- [RM03] Rossetto V & Maggs A C: Writhing geometry of Open DNA. *J. Chem. Phys.*, **118**, 9864–9874 (2003)
- [RK96] Rust D M & Kumar A: Evidence for helically kinked magnetic flux ropes in solar eruptions. *Astrophys. J. Lett.*, **464**, L199–L202 (1996)
- [S05] Starostin E L: On the writhing number of a non-closed curve. In: Calvo J, Millett K, Rawdon E, & Stasiak A (eds) *Physical and Numerical Models in Knot Theory Including Applications to the Life Sciences*. Series on Knots and Everything, World Scientific Publishing, Singapore 525–545 (2005)
- [TK05] Török T & Kliem B: Confined and ejective eruptions of kink-unstable flux ropes. *Astrophysical J.*, **630**, L97–L100 (2005)
- [VT00] van der Heijden G H M & Thompson J M T: Helical and localised buckling in twisted rods: A unified analysis of the symmetric case. *Nonlinear Dynamics*, **21**, 71–99 (2000)
- [VM97] Vologodskii A V & Marko J F: Extension of torsionally stressed DNA by external force. *Biophys. J.*, **73**, 123–132 (1997)

Random Polymers

École d'Été de Probabilités de Saint-Flour XXXVII – 2007

den Hollander, F.

2009, XIV, 266 p. 84 illus., Softcover

ISBN: 978-3-642-00332-5